

Short Communication: Fast Coriolis Mass Flow Metering for Monitoring Diesel Fuel Injection

Felix Leach, Salah Karout, Feibiao Zhou, Michael Tombs, Martin Davy, Manus Henry, University of Oxford.

Corresponding Author: Manus Henry
Department of Engineering Science
Parks Road, Oxford OX1 3PJ.
Tel +44 1865 273913
Fax +44 1865 273021
manus.henry@eng.ox.ac.uk

Abstract

Prism signal processing is a new recursive FIR technique that facilitates the rapid tracking of sinusoidal signals, such as those used in a Coriolis Mass Flow Meter (CMFM). A Prism-based CMFM prototype has been developed using a commercial flowtube and a dual ARM processor-based transmitter, which is capable of generating flow measurement updates at 48 kHz. This has been applied in a feasibility study to the tracking of fast (e.g. 1.5 ms) injections of diesel fuel on a laboratory rig at engine speeds of up to 4000 rpm equivalent and at fuel pressures of up to 100 MPa. Due to the high level of vibration in the system, Prism-based notch filtering is used to suppress undesired modes of flowtube vibration in the sensor signal. Individual flow pulses can be detected by the system, but the relatively long period of oscillation of the flowtube compared to the fuel injection duration results in a spreading out over time of each flow pulse measurement. More precise measurement results may be obtained using a higher frequency resonant flowtube.

Keywords: Prism signal processing; recursive FIR filtering; Coriolis mass flow metering; engine fuel injection monitoring; dynamic response.

[Main text begins]

One important aspect of CMFM development over recent years (see [1], particularly section 2.3.3) has been the generation of flow measurement data with high update rates (i.e. increasing the number of new measurement values generated per second) and with a rapid dynamic response (i.e. reducing the delay between a change in the true flow rate and the corresponding change in the reported measurement output). There are two primary influences on the dynamic performance of a flowmeter [2]:

- The response of the flowtube transducer, which is a function of its resonant frequencies (primarily the actively driven mode, but also its other natural modes of vibration).
- The signal processing technique applied in the electronic transmitter – for example its associated delay and its frequency response.

A third issue, measurement communication delay (typically from the transmitter to a higher level system), is important for real-time control applications but is not considered further here.

Typically [2], a commercial CMFM provides measurement update rates of up to 10 Hz, while some offer special operating modes with updates at (say) 100 Hz. In [3], an “ultrafast” prototype transmitter generates a measurement twice every drive cycle, working with a high frequency straight geometry flowtube. This provides updates at approximately 1500 Hz; experiments demonstrated a step change delay of 4 ms, and an ability to track mass flow oscillations with frequencies of up to 28 Hz.

Here we report on a new transmitter prototype incorporating Prism signal processing, which facilitates the generation of new measurement values every sample. The current prototype is based around the Zynq-7000 chip [4], in which one of the two ARM Cortex-A9 processors is dedicated to measurement calculation, and where data is sampled and measurement values are generated at 48 kHz. This prototype has a number of useful characteristics which will be discussed in further papers. However, in this short communication we reserve discussion to its application to diesel fuel injection monitoring.

Given the high pressure (up to say 300 MPa) and short duration (1 ms or less) of fuel injection pulses used in a diesel engine, it is unsurprising that direct, real-time mass flow measurement of such pulses has not

previously been reported. Existing methods of measurement are costly, and off-engine (hence not in real time), and rely on measuring pressure changes as fuel is injected into a plenum [5, 6]. However, such measurement, whether in laboratory test engines or ultimately in a commercially produced vehicle, could be valuable in detecting such defects as fuel supply imbalance to the cylinders (for example due to fuel injector deposits) and will be essential as technologies such as digital rate shaping of injections begin to see significant deployment in the automotive industry. In addition, accurate information about rate of fuel injection is essential for CFD models of combustion [7]. Overall such measurements should lead to improved efficiency and reduced emissions.

The Prism (Fig. 1) is a signal processing block accepting an input time series $s(t)$ and generating one, or more usually two, output time series, $G_s(t)$ and/or $G_c(t)$. The Prism can be viewed as a pair of FIR filters operating over a window of the input data $s(t)$ of duration $2/m$, where m is the characteristic frequency of the Prism. Unusually for an FIR filter, the Prism has a recursive calculation, so that the computational effort needed per sample is small, and is independent of the Prism sample length. This facilitates high data throughput for a given computational budget. Details of the Prism calculation will be given in a later publication.

For a steady sinusoidal input with amplitude A , frequency f and initial phase ϕ_i (i.e. the phase at $t = 0$)

$$s(t) = A \sin(2\pi f t + \phi_i), \quad (1)$$

the Prism outputs $G_s(t)$ and $G_c(t)$ are as follows:

$$G_s(t) = A \operatorname{sinc}^2(r) \frac{r^2}{r^2 - 1} \sin(\phi(t) - 2\pi r) \quad (2)$$

and

$$G_c(t) = A \operatorname{sinc}^2(r) \frac{r}{r^2 - 1} \cos(\phi(t) - 2\pi r), \quad (3)$$

where the instantaneous phase $\phi(t) = 2\pi f t + \phi_i$; $r = f/m$, the frequency ratio; and $\operatorname{sinc}(x)$ is the normalized sinc function. A second design parameter for the Prism, the harmonic number h , is a small positive integer; here it is assumed to take the value 1. The Prism outputs have linear phase delay, while the gains of $G_s(t)$ and $G_c(t)$,

labelled Γ_s and Γ_c respectively, are shown in Fig. 2; these exhibit a generally low pass characteristic with periodic notches at multiples of m , including at zero hertz.

The two Prism outputs $G_s(t)$ and $G_c(t)$ are orthogonal (i.e. a sine/cosine pair), and other than a scaling factor $1/r$, they form an analytic function from which sample-by-sample estimates of frequency, amplitude and phase may be derived. In other words, given an input signal with unknown sinusoidal properties, which is passed through a Prism with characteristic frequency m , the signal's sinusoidal properties may be estimated based on the outputs of the Prism $G_s(t)$ and $G_c(t)$. This tracking task can be performed by the Recursive Signal Tracker (RST) which employs a single Prism and recent history of $G_s(t)$ and $G_c(t)$ (Fig. 3). From an initial 'guess' (for example the value calculated from the previous sample) of r (i.e. f/m), the phase of the input signal is calculated for the current time and at $1/m$ seconds earlier; the change in phase over this known time period provides a new estimate of r and hence f , A and ϕ . This calculation is performed as follows.

Given an initial estimate of r , \hat{r} , estimates of the signal phase for the most recent sample, ϕ_0 and the sample $1/m$ seconds earlier, ϕ_m , are calculated from the recorded values of $G_s(t)$ and $G_c(t)$ using:

$$\hat{\phi}_0 = \text{atan2}(G_{s0}, \hat{r}G_{c0}) + \pi(2\hat{r} + 1) \quad (4)$$

$$\hat{\phi}_m = \text{atan2}(G_{sm}, \hat{r}G_{cm}) + \pi(2\hat{r} + 1). \quad (5)$$

Here the subscript 0 indicates data from the most recent sample, and the subscript m indicates data $1/m$ seconds earlier. From these phase values an improved value of \hat{r} can be derived using

$$\hat{r} = (\hat{\phi}_0 - \hat{\phi}_m) / 2\pi \quad (6)$$

The above steps can be repeated if required to converge onto a value for \hat{r} , but iteration is rarely required other than when tracking is initialised. With an updated value of \hat{r} , the corresponding values of f and A are given by

$$\hat{f} = \hat{r}m \quad (7)$$

$$\hat{A} = \left[\frac{\pi}{\sin(\pi\hat{r})} \right]^2 \left[1 - \hat{r}^2 \right] \sqrt{G_{s0}^2 + \hat{r}^2 G_{c0}^2} \quad (8)$$

while a final estimate of ϕ_0 may be re-calculated if required using equation (4). In the case of a CMFM, two sinusoidal sensor signals are tracked, and the phase difference, from which the mass flow is derived, may be calculated from the difference between the phases on each of the sensor signals [8].

While a standalone tracker is sufficient for monitoring a pure sinusoid contained within moderate levels of white noise, a chain of Prisms can be introduced into the signal processing path to perform pre-filtering tasks, such as low pass, bandpass and/or notch filtering. For example, Fig. 4 shows a signal processing chain consisting of two Prisms with characteristic frequencies m_1 and m_2 providing pre-filtering ahead of an RST. Such an arrangement can be used to notch out undesired frequency components at m_1 and m_2 along with all multiples of these frequencies. It is straightforward to provide phase and amplitude compensation for any pre-filtering stages.

Particularly in high vibration environments, the CMFM sensor signals may be contaminated by frequency components corresponding to undesired modes of flowtube vibration, excited by the high level of mechanical noise. Where these frequencies are steady and known (for example, when the fluid density and temperature are expected to be reasonably constant), then a simple Prism-based notch filtering arrangement can provide an effective means of removing their influence. The upper plot in Fig. 5 shows the spectrum of one of sensor signals for the CMFM flowtube used in the diesel injection experiments (Rheonik RHM 015, rated to 110 MPa); the other sensor signal has very similar properties. The highest peak, at approximately 148.8 Hz, corresponds to the actively driven mode of vibration; harmonics of this peak are present at approximately 300 Hz, 450 Hz etc. However, other prominent peaks are visible, particularly at 244.4 Hz and 261.5 Hz (and their multiples); these correspond to undesired modes of vibration. The upper plot of Fig. 5 also shows the design of the notch filter created by using the two Prisms shown in Fig. 4, where the values of m_1 and m_2 are selected to be 244.4Hz and 261.5 Hz respectively. The lower plot of Fig. 5 shows the spectrum of the sensor signal after passing through the dual Prism notch filter: the undesired vibrational modes have been successfully suppressed. In addition both very low and very high frequency components have been attenuated by the filter envelope.

The diesel fuel injection experimental set up is shown in Fig. 6. The fuel line is pressurised up to 100 MPa; in the experimental data shown here the operating pressure is 50 MPa. The fuel flow is controlled by a

prototype single-hole diesel injector known as ECN Spray A [9], which discharges fuel into a transparent cylinder. The CMFM flowtube is positioned directly upstream of the injector inlet, between the fuel rail and the injector, to monitor the liquid flow. A prototype transmitter maintains flowtube operation and generates in real time, using the Prism signal processing scheme shown in Fig. 4, the observed flow rate (shown here simply as phase difference between the two sensor signals). The sensor signals are sampled at 48 kHz, and flow measurement data is generated at the same rate. The value of m for the RST shown in Fig. 4 is 297.6 Hz, which results in an optimal value of $r = 0.5$ for a flowtube resonant frequency of 148.8 Hz. The transmitter has sufficient local memory to record up to 50s of data at full bandwidth, including raw sensor data and the calculated sinusoidal parameters. The data can subsequently be downloaded to allow data visualisation and further analysis.

Fig. 7 shows experimental results in which a sequence of regularly spaced 1.5 ms fuel pulses is passed through the flowmeter at 15 Hz (corresponding to an engine speed in a four-stroke engine of 1800 rpm). In the upper plot, the live results are compared with off-line processing of the sensor data in which the notch filtering is not applied. This comparison demonstrates the utility of the notch filtering – without it no useful flow measurement data could be obtained. The lower plot shows the filtered results only: each fuel pulse is clearly discernable. Fig. 8 shows two of the fuel pulses in greater detail. Note that the peak phase difference for each fuel pulse, at around 0.45 degrees, corresponds to a mass flow rate of approximately 3 g/s based on the flowtube calibration at low pressure conditions. This broadly matches the expected peak flow rate from the injector. However, the true duration of each fuel pulse is 1.5 ms but in the measurement data this has been extended over a time period of approximately 16 ms. Correspondingly, the totalized mass over each pulse is approximately 20 mg, a significant over-read compared with the expected value of around 4 mg. This spreading out of each fuel pulse in time is attributable to both the physical response of the flowtube, and the dynamic response of the transmitter, where the signal processing scheme (e.g. the value of m) is designed to match the flowtube oscillation frequency. Other results (not shown) indicate that for these very short flow events the peak observed flowrate is a function of the phase of flowtube oscillation. For example, the roughly linear change in peak heights observed in Figure 7 is at least partly attributable to fact that the 15 Hz pulse injection rate is approximately (but not exactly) 10 times the flowtube resonant frequency, resulting in a low frequency beating

effect. Again, the most straightforward means of attenuating this effect in our future research is to utilize a flowtube with a significantly higher resonant frequency.

These provisional results are presented as a first demonstration of capability. Many important technical issues remain to be resolved, for example the development of a metrological standard for calibrating flow metering in high pressure and with very short flow pulses. High pressure calibration facilities are being developed in support of hydrogen fuel applications [10], while pressure effects on CMFMs are a continuing research topic [11]. Note also that CMFMs are already used to monitor the *average* fuel flow rate supplied to laboratory engines. However, the very short batch duration compared with the period of the flowtube appears to be the most significant measurement challenge, and in our future research we will seek to improve dynamic performance by selecting/designing/adapting flowtubes to operate at higher frequencies (ideally 1 kHz or above), despite the additional challenges of high pressure and high mechanical noise. If this leads to a significant reduction in the time ‘spreading’ of the fuel pulses, then it is hoped that a reasonable calibration can be achieved using an averaged flow rate from a reference meter.

Acknowledgement

The work described in this paper was supported by funding from the Advanced Propulsion Centre Ltd, UK (grant number: PGC015) and Rheonik, Germany.

References

- [1] Wang, T, and Baker, R. "Coriolis flowmeters: a review of developments over the past 20 years, and an assessment of the state of the art and likely future directions", Flow Measurement and Instrumentation 40 (2014), pp99–123. DOI: <http://dx.doi.org/10.1016/j.flowmeasinst.2014.08.015>
- [2] Henry MP, Clark C, Duta M, Cheesewright R, Tombs M S. Response of a Coriolis mass flow meter to step changes in flow rate. Flow Measurement and Instrumentation 2003;14:109–18. DOI: [https://doi.org/10.1016/S0955-5986\(03\)00014-1](https://doi.org/10.1016/S0955-5986(03)00014-1)
- [3] Clark C, Zamora M, Cheesewright R, Henry M. The dynamic performance of a new ultra-fast response Coriolis flow meter. Flow Measurement and Instrumentation 2006;17:391–8. DOI: <https://doi.org/10.1016/j.flowmeasinst.2006.07.002>
- [4] Xilinx, <https://www.xilinx.com/products/silicon-devices/soc/zynq-7000.html>
- [5] Arcoumanis, C. and M.S. Baniasad, Analysis of Consecutive Fuel Injection Rate Signals Obtained by the Zeuch and Bosch Methods. 1993, SAE International.
- [6] Marčič, M., Measuring method for diesel multihole injection nozzles. Sensors and Actuators A: Physical, 2003. 107(2): p. 152-158.
- [7] Leach, F., Ismail, R., Davy, M., Weall, A. et al., "Comparing the Effect of Fuel/Air Interactions in a Modern High-Speed Light-Duty Diesel Engine," SAE Technical Paper 2017-24-0075, 2017. DOI: 10.4271/2017-24-0075
- [8] M.P Henry, D.W Clarke, N Archer, J Bowles, M.J Leahy, R.P Liu, J Vignos, F.B Zhou, A self-validating digital Coriolis mass-flow meter: an overview, Control Engineering Practice, Volume 8, Issue 5, May 2000, Pages 487-506, ISSN 0967-0661, [https://doi.org/10.1016/S0967-0661\(99\)00177-X](https://doi.org/10.1016/S0967-0661(99)00177-X).
- [9] Bardi, M., et al., ENGINE COMBUSTION NETWORK: COMPARISON OF SPRAY DEVELOPMENT, VAPORIZATION, AND COMBUSTION IN DIFFERENT COMBUSTION VESSELS. Atomization and Sprays, 2012. 22(10): p. 807-842. <https://doi.org/10.1615/AtomizSpr.2013005837>

[10] T. Morioka, M. Ito, S. Fujikawa, M. Ishibashi, S. Nakao. “Development and evaluation of the calibration facility for high-pressure hydrogen gas flow meters”, Flow Measurement and Instrumentation, Volume 39, 2014, Pages 19-24, ISSN 0955-5986, <http://dx.doi.org/10.1016/j.flowmeasinst.2014.05.019>.

[11] T. Wang, Y. Hussain. “Pressure effects on Coriolis mass flowmeters”, Flow Measurement and Instrumentation, Volume 21, Issue 4, 2010, Pages 504-510, ISSN 0955-5986, <http://dx.doi.org/10.1016/j.flowmeasinst.2010.08.001>.

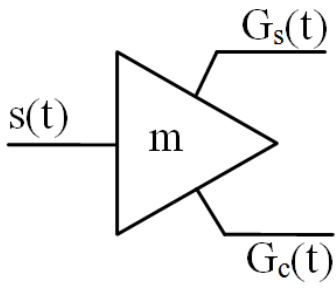


Figure 1. Prism signal processing block with time series input $s(t)$ and time series outputs $G_s(t)$ and $G_c(t)$.

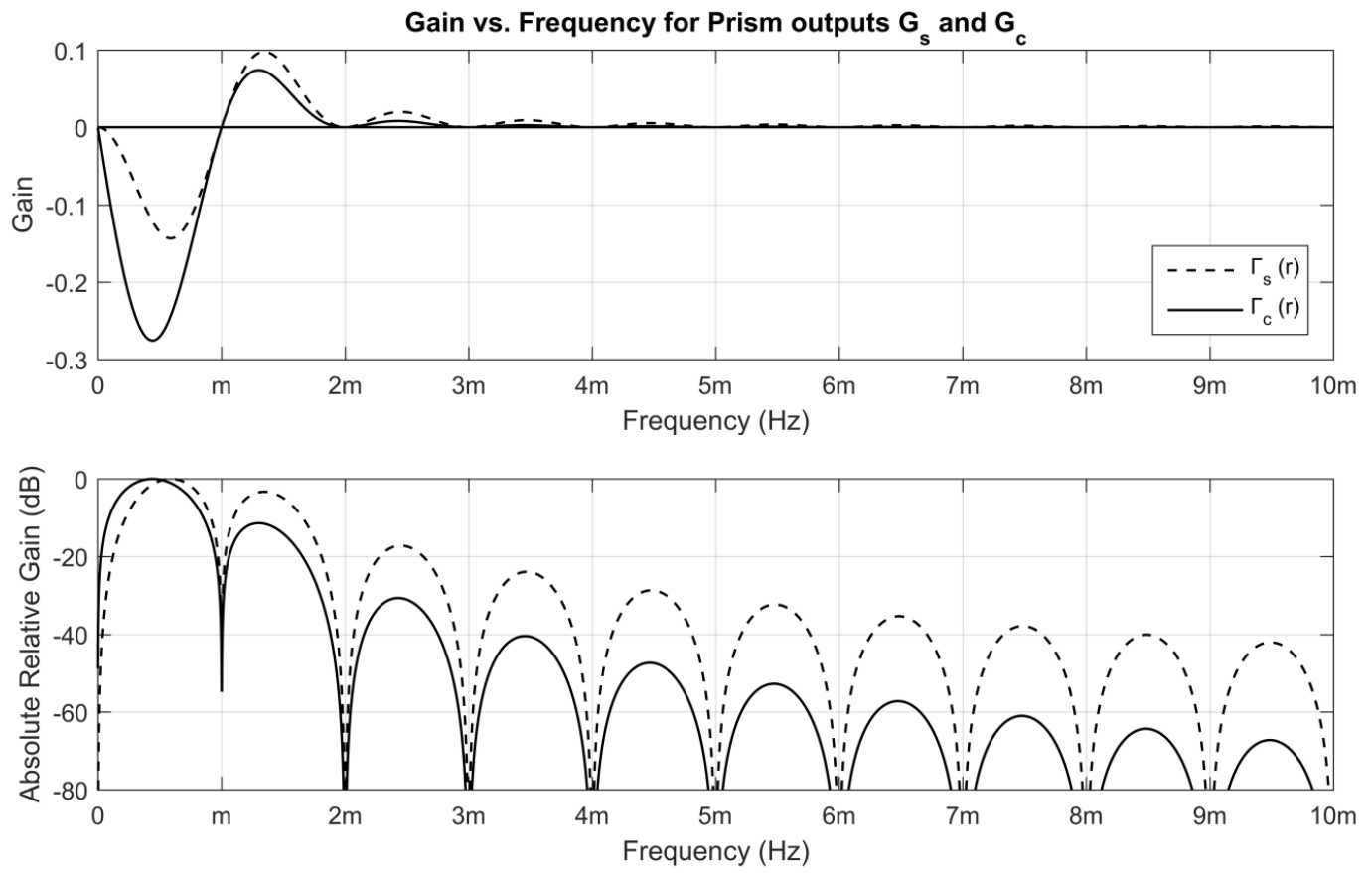


Figure 2. Gains of Prism outputs $G_s(t)$ and $G_c(t)$.

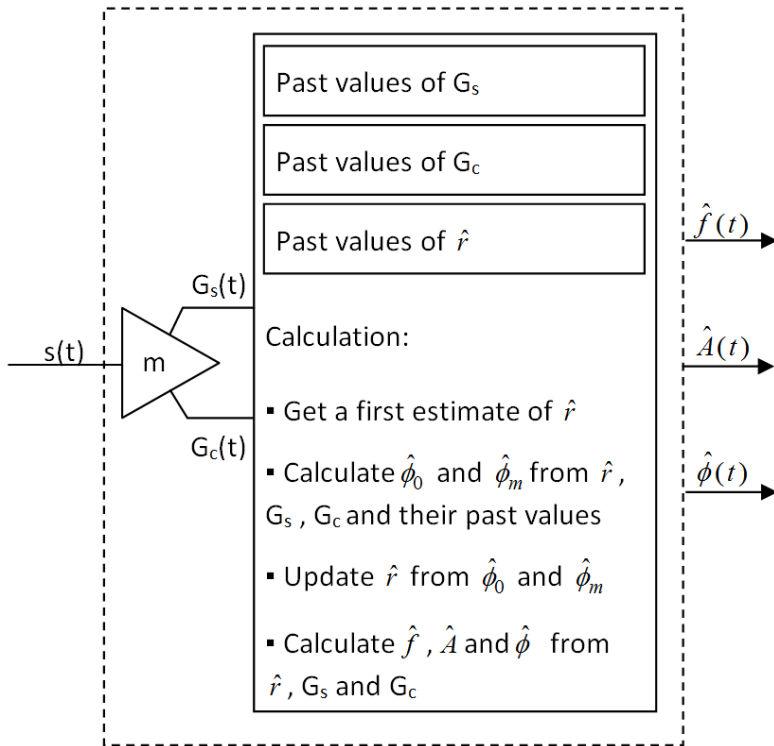


Figure 3. Recursive Signal Tracker (RST)

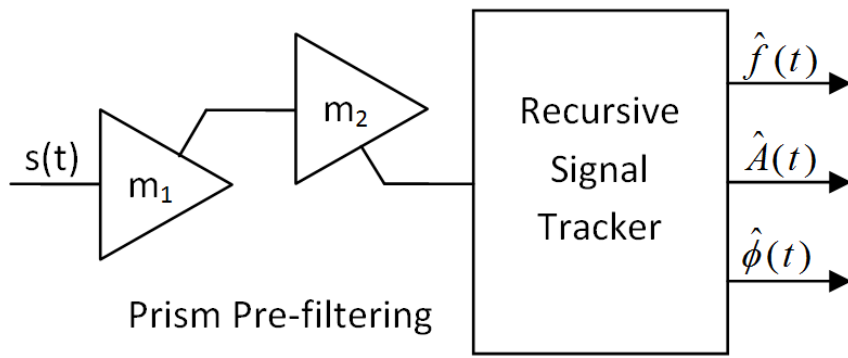


Figure 4. Signal tracking with pre-filtering

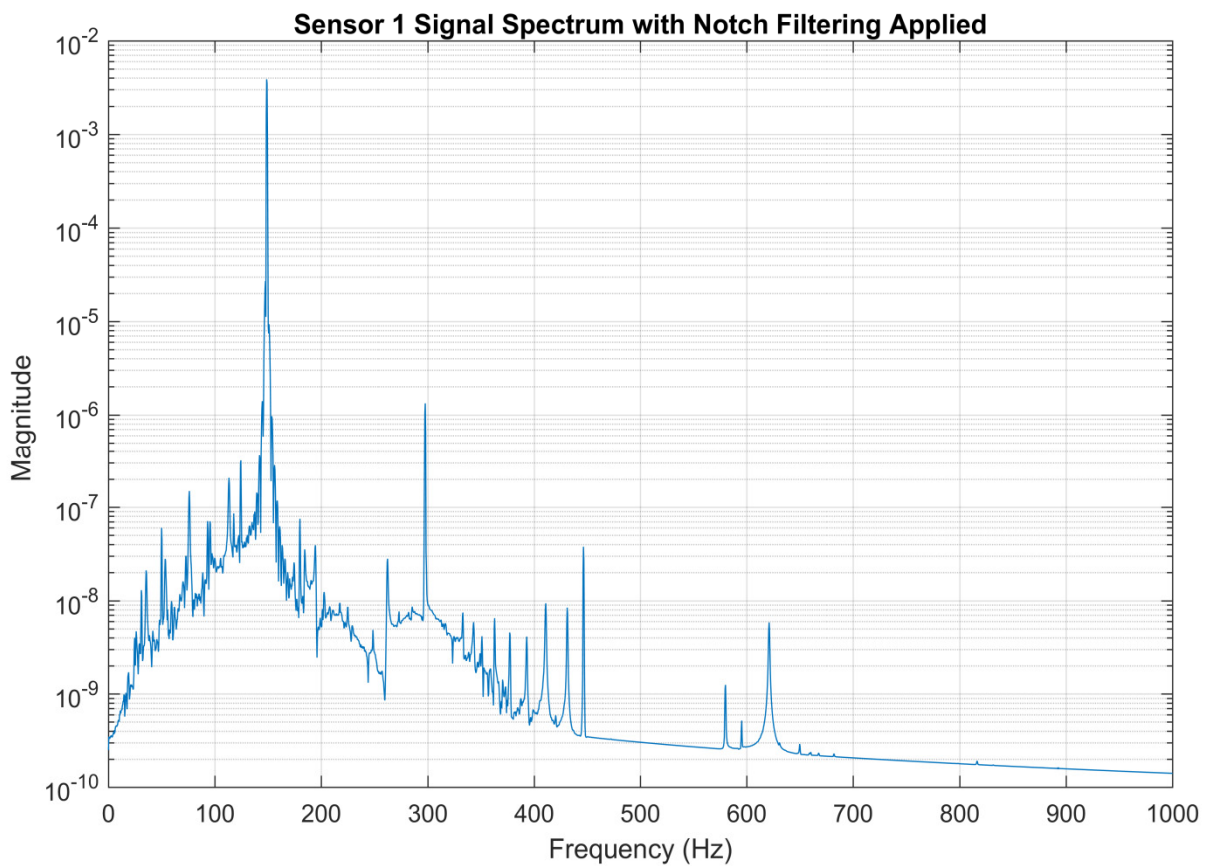
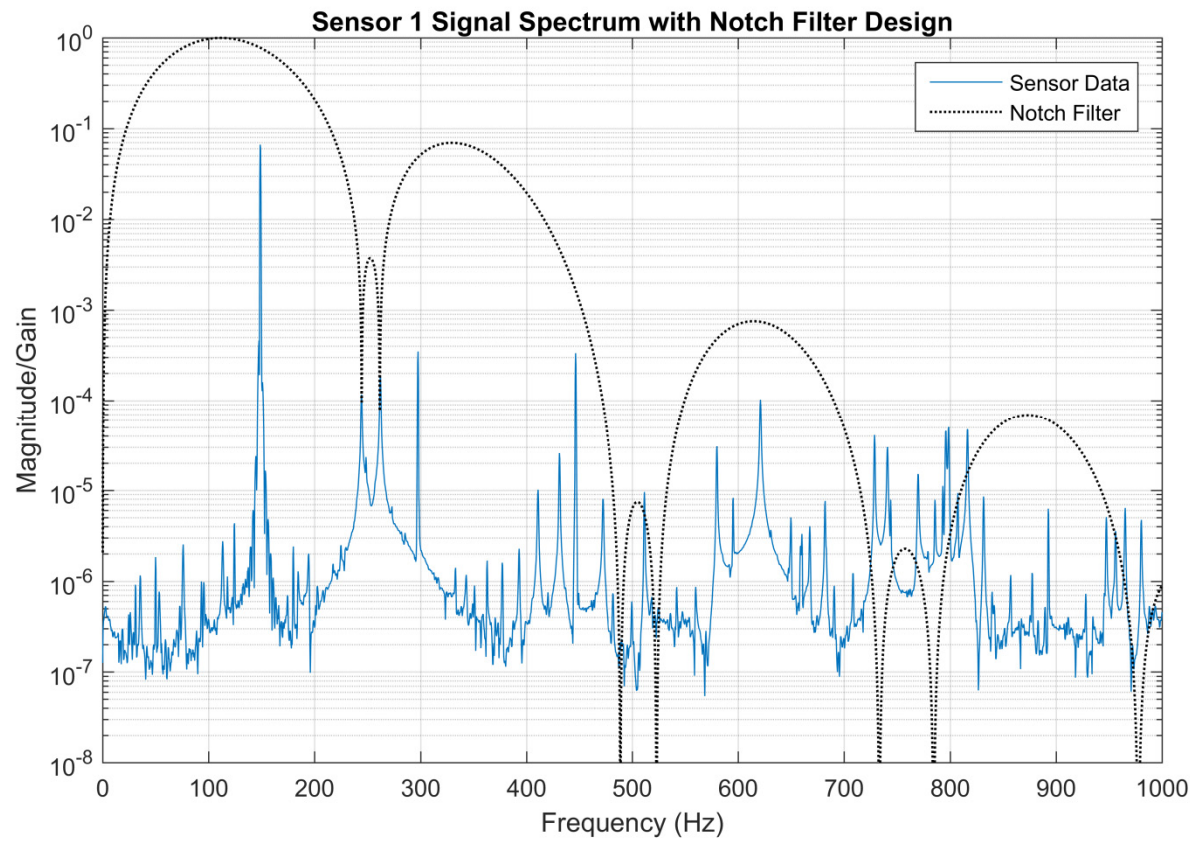


Figure 5: Coriolis sensor signal power spectrum: (upper) raw data and Prism-based notch filter design; (lower) filtered sensor signal.

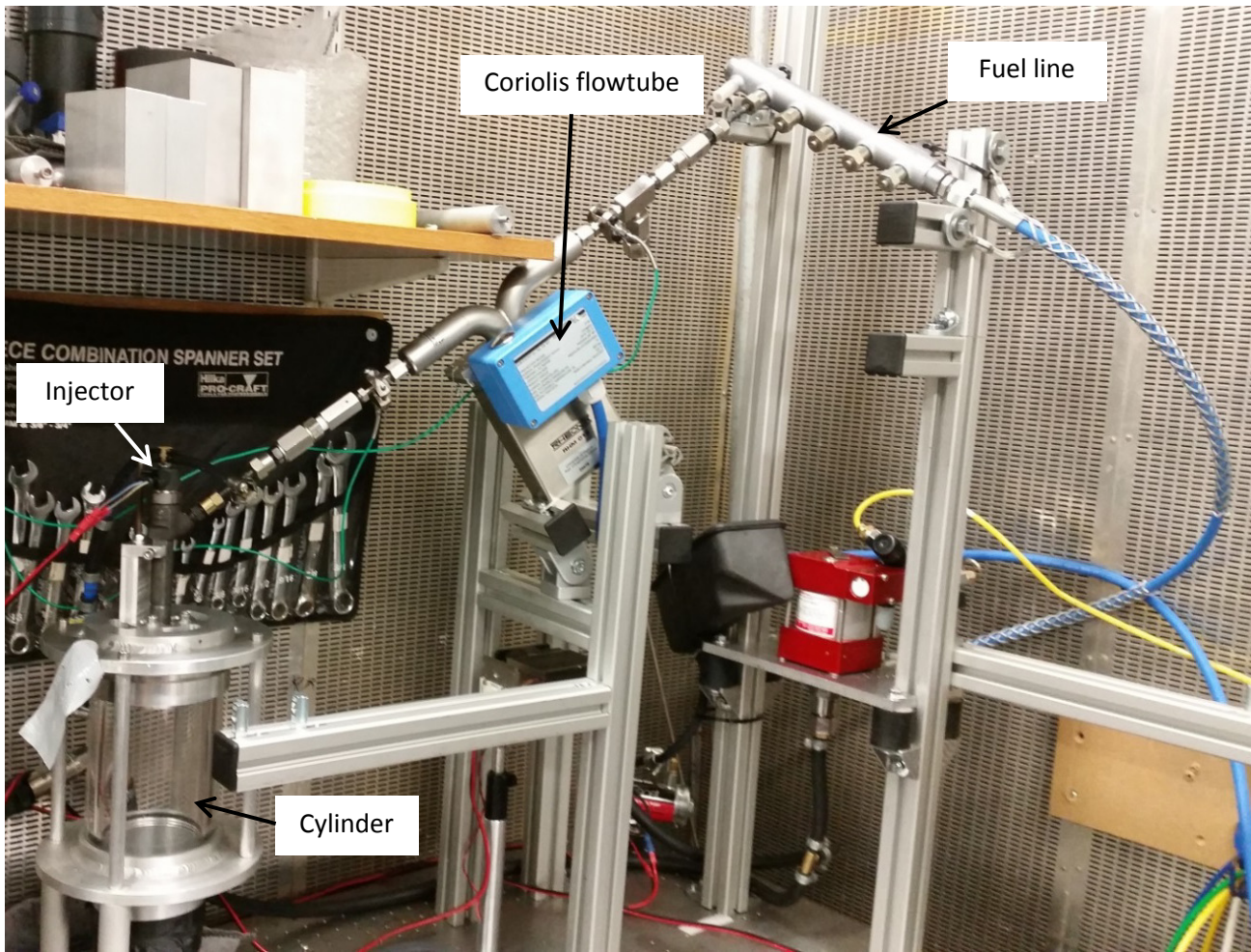


Figure 6: Experimental setup

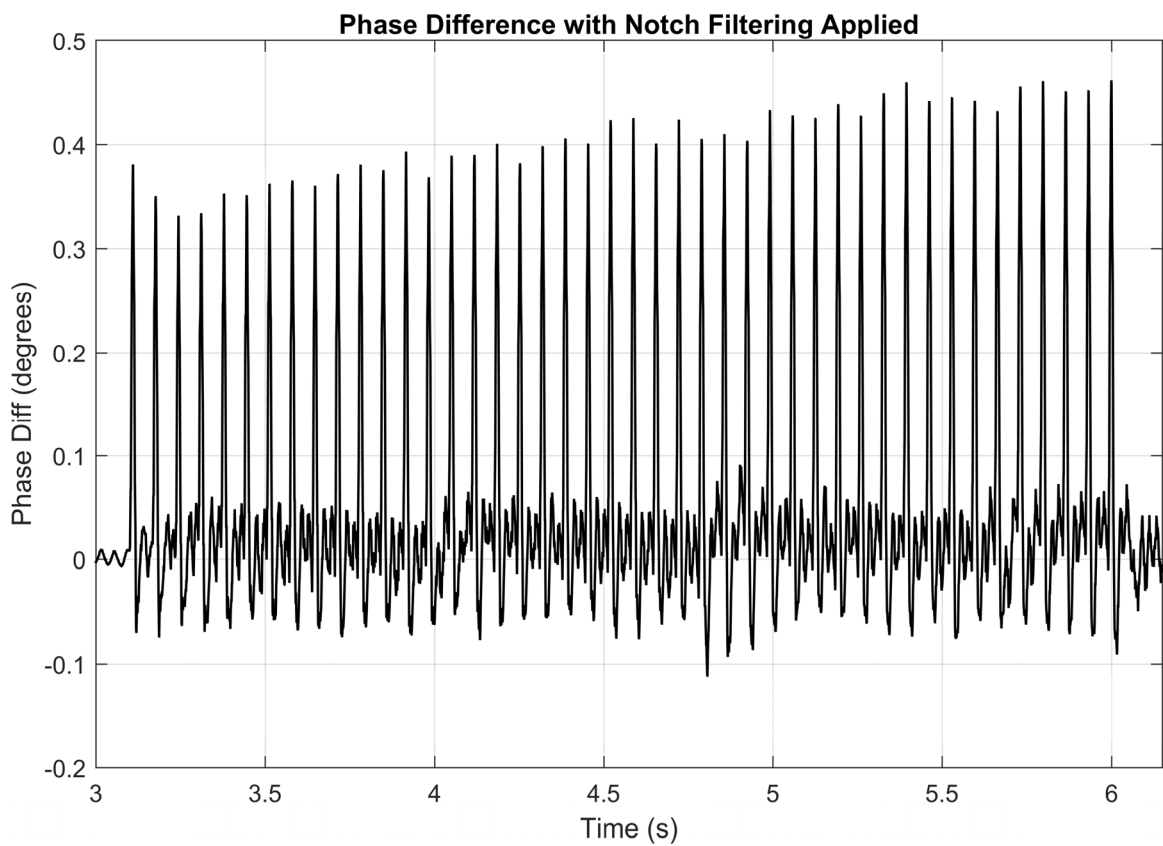
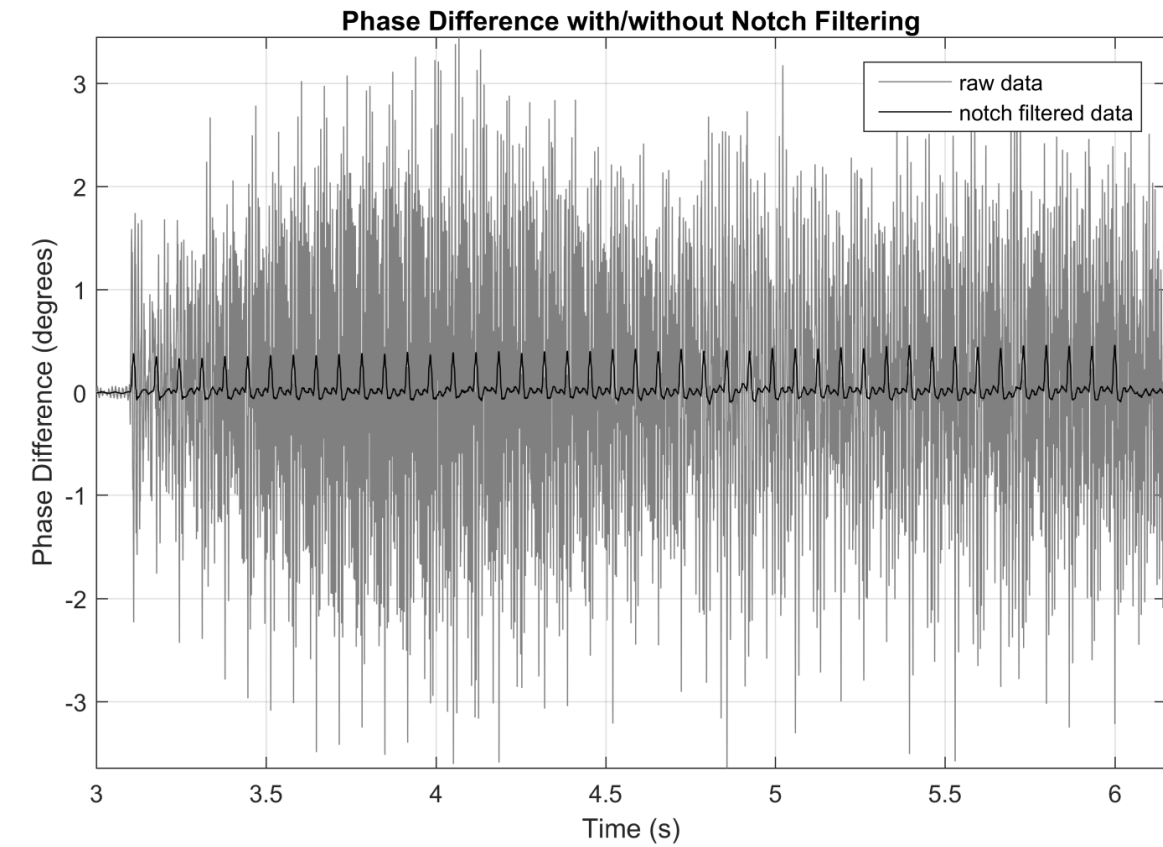


Figure 7: Phase difference calculation during diesel fuel injection: (upper) raw and notch filtered data compared; (lower) notch filtered data only.

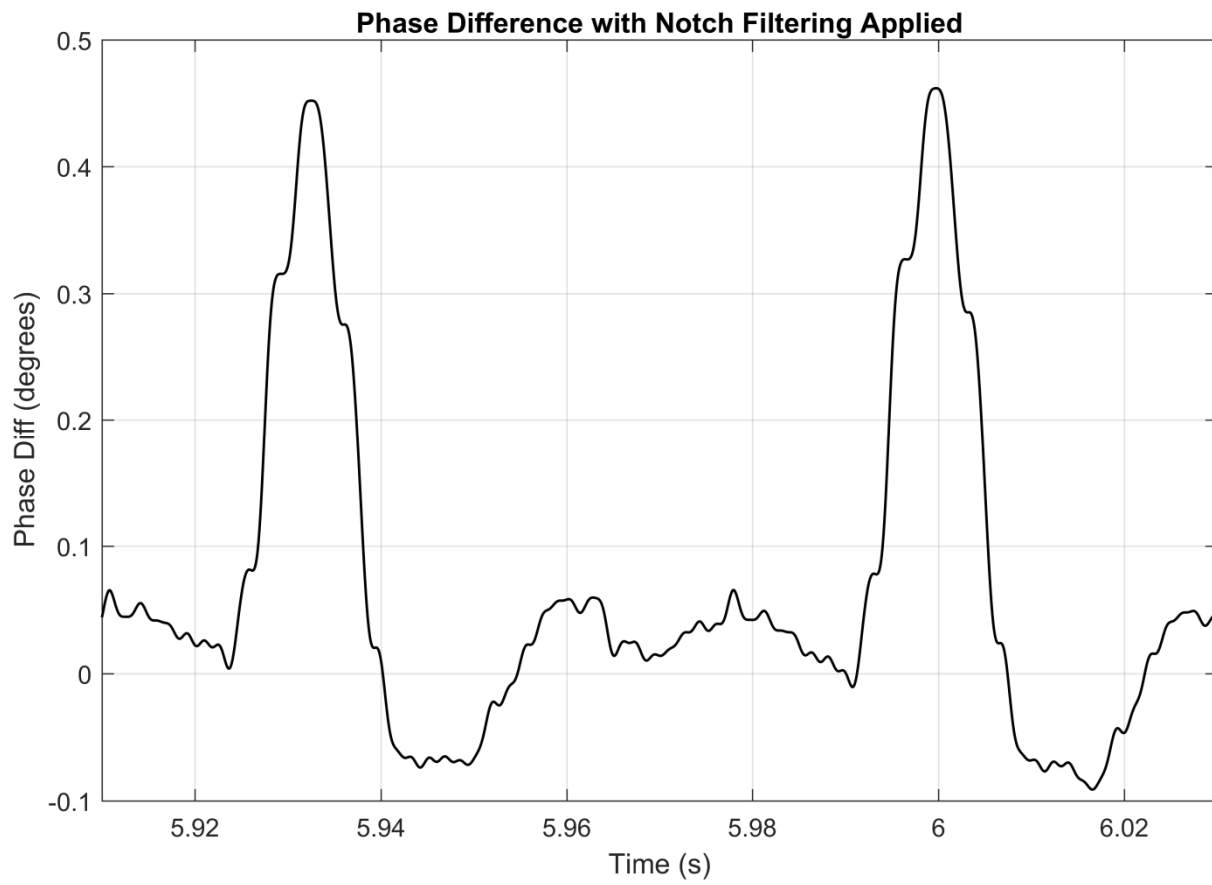


Figure 8: Recorded measurement of consecutive fuel pulses (detail).